

Polymer Chemistry

Accepted Manuscript



This is an *Accepted Manuscript*, which has been through the Royal Society of Chemistry peer review process and has been accepted for publication.

Accepted Manuscripts are published online shortly after acceptance, before technical editing, formatting and proof reading. Using this free service, authors can make their results available to the community, in citable form, before we publish the edited article. We will replace this *Accepted Manuscript* with the edited and formatted *Advance Article* as soon as it is available.

You can find more information about *Accepted Manuscripts* in the [Information for Authors](#).

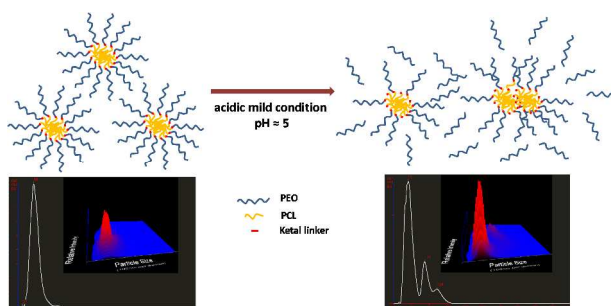
Please note that technical editing may introduce minor changes to the text and/or graphics, which may alter content. The journal's standard [Terms & Conditions](#) and the [Ethical guidelines](#) still apply. In no event shall the Royal Society of Chemistry be held responsible for any errors or omissions in this *Accepted Manuscript* or any consequences arising from the use of any information it contains.

TOC - Graphical Abstract

(For Table of Contents Use Only)

Novel poly(ethylene oxide monomethyl ether)-*b*-poly(ϵ -caprolactone) diblock copolymers containing a pH-acid labile ketal group as blocks linkage

S. Petrova,* E. Jäger, R. Konefał, A. Jäger, C. G. Venturini, J. Spěváček, E. Pavlova and P. Štěpánek



Acidic physiological conditions trigger degradation of amphiphilic block copolymers containing a ketal group as block linkage into biocompatible degradation products.

Novel poly(ethylene oxide monomethyl ether)-*b*-poly(ϵ -caprolactone) diblock copolymers containing a pH-acid labile ketal group as a block linkage

Cite this: DOI: 10.1039/x0xx00000x

Received 00th January 2012,
Accepted 00th January 2012

DOI: 10.1039/x0xx00000x

www.rsc.org/

S. Petrova*, E. Jäger, R. Konefał, A. Jäger, C. G. Venturini, J. Spěvák, E. Pavlova and P. Štěpánek

A new biocompatible and biodegradable diblock copolymer that contains a specific acid-labile degradable linkage (acyclic ketal group) between the hydrophobic poly(ϵ -caprolactone) (PCL) and the hydrophilic poly(ethylene oxide monomethyl ether) (MPEO) blocks is described herein. A multi-step synthetic method that combines carbodiimide chemistry, a “click” reaction and ring-opening polymerisation (ROP) was employed to successfully produce a series of MPEO-*b*-PCL diblock copolymers (herein referred to as MPEO₄₄-*b*-PCL₁₇ and MPEO₄₄-*b*-PCL₄₄). 2-[[2-(2-Azidoethoxy)propan-2-yl]ethan-1-ol was obtained as a linker between the two blocks through a three-step synthetic approach. Furthermore, a newly developed α -methoxy- ω -hydroxy-poly(ethylene oxide) that contains an acid-labile ketal linkage was designed as a macroinitiator *via* a “click” reaction for the sequential controlled ring-opening polymerisation of ϵ -CL. The newly obtained compounds (precursors, macromer, macroinitiator and final diblock copolymers) were assessed using ¹H NMR, ¹³C NMR and FT-IR spectroscopy and SEC analysis, which are described in this manuscript. Upon dissolution in a mild organic solvent, the MPEO₄₄-*b*-PCL₁₇ block copolymer self-assembled in water/PBS into regular, spherical, stable nanoparticles (NPs). Furthermore, the presence of the acid-labile ketal linker enabled the disassembly of these nanoparticles in a buffer that simulated acidic cytosolic or endosomal conditions in tumour cells as evaluated by dynamic light scattering (DLS), nanoparticle tracking analysis (NTA) and transmission electron microscopy (TEM) images. This disassembly led to hydrolysis profiles that resulted in neutral degradation products.

Introduction

Currently, the priorities for the development of polymer therapeutics are strictly associated with the production of biocompatible, degradable polymeric nanostructures. The properties of these materials are defined by their structures, compositions, dimensions and functionalities. Over the past several decades, amphiphilic block copolymers (hydrophilic and hydrophobic blocks) have been extensively studied.¹⁻⁴ These copolymers are of great interest because of their ability to self-assemble in aqueous media to generate various structure types, shapes and sizes, ranging from nano- to micrometres.⁵⁻⁷ It is well known that amphiphilic block copolymers are able to form nanosized spherical micelles with a core-shell architecture. The applications for these systems are associated with their several unique properties, such as the possibility of controlling the release of drugs,⁸⁻¹⁰ matrices for three-dimensional tissue regeneration,¹¹⁻¹³ diagnostic agents^{14,15} and DNA delivery^{16,17}. In particular, self-assembled core-shell NPs from amphiphilic block copolymers have attracted considerable attention in the development of drug-delivery systems. Their hydrophobic core is used as a reservoir for lipophilic agents

(drugs), whereas their hydrophilic corona creates a highly water-bound barrier that ensures colloidal stability, a reduction in the rate of opsonin adhesion and clearance of the particles from the body.¹⁸ Another relevant consideration for the development of core-shell NPs for drug-release applications is the carriers' ability to release their cargo drug in a controlled manner upon arrival at the target site.¹⁹ For these reasons, many researchers are placing special attention on the design of environmentally triggered polymeric nanoparticles that are capable of releasing the original molecules in their active forms under various chemical and physical stimuli, such as pH, light, temperature, enzyme concentration or redox gradients.²⁰⁻²² pH-sensitive degradable polymers have played an integral role in the advancement of drug-delivery technology, such as the delivery of protein-based vaccines and nucleic acids, in the treatment of acute inflammatory diseases and especially for tumour targeting.^{23,24} Considering the tumour-targeting field of drug delivery, the hydrophobic guest drug molecules must be retained in the inner particle core while in the bloodstream and then be rapidly released at the specific tumour sites.²⁵ Considerable research has demonstrated the association between acidic pH conditions and cancer, as the extracellular

pH in most solid tumour sites is more acidic (ranging from pH 5.7 to 7.2) compared to that of normal tissues (buffered at pH 7.4).^{26,27} Because of these pH differences, several pH-degradable polymers that contain different acid-labile linkers suitable for triggering drug release, such as ester,²⁸ hydrazone,²⁹ carboxydimethylmaleic,³⁰ orthoester,³¹ imine,³² β -thiopropionate,³³ vinyl ether,³⁴ and phosphoramidate,³⁵ have been widely studied. In particular, acid-degradable (co)polymers and NPs that contain multiple reactive functionalities, such as ketal/acetal labile linkages along the polymer backbone or as pendant groups, are of considerable interest. Ketals and acetals have been demonstrated to be more sensitive to the acidic environment of tumours and phagosomes than esters and hydrazones.³⁵ Moreover, these linkers are also more stable under physiological conditions (at pH \sim 7.4) than the other aforementioned linkages.³⁶ In addition, pH-responsive systems containing acid-labile bonds that are degradable under mild acidic conditions, such as those of tumour sites, lead to tuneable hydrolysis profiles, which ultimately result in neutral degradation products that can be easily excreted, thereby avoiding accumulation and inflammatory responses.³⁷ Although novel and efficient pH-sensitive carriers that contain ketal/acetal linkages have great potential for drug delivery, synthetic challenges have limited the applications of these systems.

Herein, we report the synthesis of a novel class of well-defined biocompatible and biodegradable acid-labile poly(ethylene oxide monomethyl ether) (MPEO)-*b*-poly(ϵ -caprolactone) (PCL) diblock copolymers that contain ketal groups as block linkers. The PEO and PCL polymers were selected as building blocks because of their special interest for environmental, biomedical and pharmaceutical applications.³⁸⁻⁴¹ PCL is an aliphatic hydrophobic polyester with great potential as a biomaterial due to its unique combination of biodegradability and biocompatibility,⁴² and PEO is a hydrophilic and very flexible biocompatible polymer that is non-toxic and easily eliminated from the body.⁴³ For the synthesis, an efficient multi-step pathway was employed, which resulted in new block copolymers with reasonable yields. Different synthetic routes (i.e., carbodiimide chemistry, "click" reaction and ring-opening polymerisation) were applied for the preparation of low-molecular-weight compounds as precursors for constructing the acid-labile ketal group of the MPEO-*b*-PCL diblock copolymers. In addition, the amphiphilic diblock copolymers self-assembled into regular spherical NPs in aqueous solution and under buffer-simulated physiological conditions (pH \sim 7.4). These nanoparticles were found to be degraded into non-toxic compounds under buffer-simulated acidic cytosolic or endosomal conditions in tumour cells (pH \sim 5.0), revealing their potential as systems that could find applications, e.g., as acid-labile drug-delivery systems.

Experimental

Materials

Ethylene glycol (99%, Sigma-Aldrich), trimethyl orthoacetate (99%, Aldrich), *p*-toluenesulphonic acid monohydrate (98.5%, Fluka), 2-chloroethanol (99%, Aldrich), sodium azide (99%, Fluka), tetrabutylammonium bromide (TBABr, 99%, Fluka), pyridinium *p*-toluenesulphonate (PPTS, 99%, Fluka), 5-hexynoic acid (97%, Aldrich), 4-dimethylaminopyridine (DMAP, 99% Sigma-Aldrich), *N,N'*-dicyclohexylcarbodiimide (DCC, 99%, Fluka), CuBr (98%, Fluka), 2-methoxypropene (98%, Aldrich), molecular sieves (5 Å, Sigma-Aldrich) and ϵ -

caprolactone (ϵ -CL, 99%, Sigma-Aldrich) were used without further purification. The ϵ -CL was dried over CaH₂ with continuous stirring at room temperature for 48 h and distilled under reduced pressure before use. Tin (II) bis(2-ethylhexanoate) (Sn(Oct)₂, 95%, Aldrich, 0.06 M solution in toluene) and sodium hydroxide (NaOH) were used as received. MPEO ($M_n \sim$ 1800 g/mol) was purchased from Fluka. Triethylamine (Et₃N) (\geq 99.5%, Sigma-Aldrich) was dried over CaH₂ and distilled under reduced pressure. CH₂Cl₂ (Sigma-Aldrich) was dried by refluxing over a benzophenone-sodium complex and distilled under an argon atmosphere. Toluene (99%, Labscan) and tetrahydrofuran (THF, 99%, Fluka) were refluxed for 24 h over CaH₂ under a dry argon atmosphere and then distilled. All other chemicals were used as received.

Synthesis of compounds 1-5

Compounds **1**,^{44,45} **2**,⁴⁶ **3**,⁴⁵ **4**,⁴⁵ and **5**⁴⁷ were synthesised according to previous procedures, which are described in detail in the Supplementary Information.

Synthesis of α -methoxy- ω -hydroxy-poly(ethylene oxide) containing a ketal group (compound 6)

The coupling of 2-([2-(2-azidoethoxy)propan-2-yl]ethan-1-ol) (**4**) (0.18 g, 7.78 \times 10⁻⁴ mol) with α -methoxy- ω -alkyne-poly(ethylene oxide) (**5**) (1.4 g, 7.09 \times 10⁻⁴ mol) bearing the alkyne was performed in a glass reactor containing dry THF (8 mL). CuI (0.015 g, 7.87 \times 10⁻⁵ mol) and triethylamine (0.01 mL, 7.91 \times 10⁻⁵ mol) were added to the polymer solution and allowed to react at 35 °C for 4 h. Subsequently, the reaction mixture was exposed to air, diluted with THF, and passed through a neutral alumina column to remove the copper catalysts. The macroinitiator was recovered by two precipitations in cooled diethyl ether. The product (**6**) was recovered as a white solid. Yield: 1.30 g, 93%.

Synthesis of MPEO-*b*-PCL diblock copolymer containing a ketal group (compound 7)

In a typical synthesis, 0.127 g (5.7 \times 10⁻⁵ mol) of α -methoxy- ω -hydroxy-poly(ethylene oxide) (**6**) containing a ketal group was introduced into a 50 mL glass reactor equipped with a magnetic stir bar. The macroinitiator was dissolved in dry toluene and dried three times by azeotropic distillation. A certain amount of freshly distilled ϵ -CL was added, and after heating, 0.1 mL of 0.06 M Sn(Oct)₂ was rapidly injected through a septum. The polymerisation was carried out for 48 h at 110 °C. The reactor was cooled to room temperature, and the reaction mixture was dissolved in toluene. The copolymer (**7**) was collected by precipitation in cooled diethyl ether, filtered and dried overnight under vacuum at 40 °C.

Characterisation Techniques

¹H NMR and ¹³C NMR spectra (300 and 75 MHz, respectively) were recorded using a Bruker Avance DPX 300 NMR spectrometer with CDCl₃ as the solvent at 25 °C. The chemical shifts are relative to TMS using hexamethyldisiloxane (HMDSO, δ = 0.05 and 2.0 ppm from TMS in ¹H NMR and ¹³C NMR spectra) as the internal standard. The M_n of compounds **5-7** were determined by ¹H NMR spectroscopy. For compound **5**, the M_n was calculated according to Eq. 1:

$$M_{n(\text{NMR})} = [(I_b/4)/(I_d/2)] \times 44 + 31 + 95 \quad (1)$$

where I_b and I_d represent the integral values of the peaks at $\delta = 3.63$ ppm ($-\text{CH}_2-\text{CH}_2-\text{O}-$ of the PEO repeating unit) and at $\delta = 4.22$ ppm ($-\text{CH}_2-\text{CH}_2-\text{O}-\text{C}(\text{O})-$), respectively. The values 31 and 95 represent the molecular weights of the two functional groups at the chain ends $\text{CH}_3-\text{O}-$ and $-\text{C}(\text{O})-\text{C}(\text{CH}_2)_3-\text{C}\equiv\text{CH}$, respectively. The M_n of the macroinitiator (**6**) was calculated according to Eq. (2):

$$M_{n(\text{NMR})} = [(I_b/4)/(I_g/2)] \times 44 + 31 + 284 \quad (2)$$

where I_b and I_g represent the integral values of the peaks at $\delta = 3.63$ ppm ($-\text{CH}_2-\text{CH}_2-\text{O}-$ of the PEO repeating unit) and at $\delta = 2.76$ ppm ($-\text{O}-\text{C}(\text{O})-\text{CH}_2-\text{CH}_2-\text{CH}_2-$), respectively. The values 31 and 284 are the molecular weights of the two functional groups at the chain ends $\text{CH}_3-\text{O}-$ and $-\text{O}-\text{C}(\text{O})-(\text{CH}_2)_3$ -triazole ring- $(\text{CH}_2)_2-\text{OC}(\text{CH}_3)_2-\text{O}-(\text{CH}_2)_2-\text{OH}$, respectively. The M_n of the MPEO-*b*-PCL diblock copolymers (**7**) were determined by ^1H NMR using Eq. (3)

$$\frac{M_{n(\text{NMR})}(\text{MPEO-}b\text{-PCL})}{M_{n(\text{NMR})}(\text{macroinitiator})} = [(I_r/2)/(I_b/4)] \times \text{DP}_{\text{MPEO}} \times 114 + \quad (3)$$

where I_r and I_b represent the integral values of the methylene protons of PCL (**r**) (Fig. 2., top) and of the methylene protons of PEO (**b**). The value 114 is the molecular weight of the ϵ -CL unit, DP_{MPEO} is the degree of polymerisation of the macroinitiator, and $M_{n(\text{NMR})}$ is the number-average molecular weight of the macroinitiator. Infrared spectra were obtained using a PerkinElmer Spectrum 100 equipped with a universal ATR (attenuated total reflectance) accessory with a diamond crystal. In all cases, the resolution was 4 cm^{-1} and the spectra were averaged over 16 scans. The samples were prepared in the form of KBr pellets. The number-average molecular weights (M_n), weight-average molecular weights (M_w), and polydispersity indices (M_w/M_n) of the prepared macromer, macroinitiator and block copolymers were determined through size exclusion chromatography (SEC). The analyses were performed using an SDS 150 pump (Watrex, Czech Republic) equipped with refractometric (Shodex RI-101, Japan) and UV (Watrex UVD 250, Czech Republic) detectors. The separation system consisted of two PLgel MIXED-C columns (Polymer Laboratories) and was calibrated with polystyrene standards (PSS, Germany). THF was used as the mobile phase at a flow rate of $1.0 \text{ mL}\cdot\text{min}^{-1}$ at 25°C . Data collection and processing were performed using the Clarity software package.

Nanoparticle preparation

NPs were prepared using the nanoprecipitation protocol. A preheated (40°C) acetone solution (5 mL) containing the MPEO-*b*-PCL block copolymer (10 mg) was added drop-wise (EW-74900-00, Cole-Parmer[®]) into a pre-heated (40°C) Milli-Q[®] water solution (10 mL, pH ~ 7.4). The pre-formed NPs were allowed to self-assemble, and then the solution was transferred to a dialysis tube (MWCO = 3500) and dialysed against 5 L of water (pH ~ 7.4) for 24 hours. The final concentration was adjusted to $1 \text{ mg}\cdot\text{mL}^{-1}$ using phosphate-buffered saline (PBS) at pH ~ 7.4 .

Nanoparticle characterisation

The NPs were characterised using DLS and NTA. The DLS measurements were performed using an ALV CGE laser goniometer consisting of a 22 mW HeNe linearly polarised laser operating at a wavelength ($\lambda = 632.8 \text{ nm}$), an ALV 6010 correlator, and a pair of

avalanche photodiodes operating in the pseudo cross-correlation mode. The samples were filtered through $0.45 \mu\text{m}$ PVDF membranes (Millex-HV, Millipore[®]) loaded into 10 mm diameter glass cells and maintained at 25 or $37 \pm 1^\circ\text{C}$. The data were collected using the ALV Correlator Control software, and the counting time was 30 s. To avoid multiple light scattering, the samples were diluted 100-fold before the measurements.⁴⁸ The measured intensity correlation functions $g_2(t)$ were analysed using the algorithm REPES (incorporated in the GENDIST program),⁴⁹ resulting in the distributions of relaxation times shown in an equal area representation as $\tau A(\tau)$. The mean relaxation time or relaxation frequency ($\Gamma = \tau^{-1}$) is related to the diffusion coefficient (D) of the nanoparticles as $D = \frac{\Gamma}{q^2}$, where $q = \frac{4\pi n \sin(\theta/2)}{\lambda}$ is the scattering

vector with n representing the refractive index of the solvent and θ representing the scattering angle. The hydrodynamic radius (R_H) or the distributions of R_H was calculated using the well-known Stokes-Einstein relation:

$$R_H = \frac{k_B T}{6\pi\eta D} \quad (4)$$

where k_B is the Boltzmann constant, T is the absolute temperature, and η is the viscosity of the solvent. The NTA analyses were performed using the NanoSight LM10 & NTA 2.0 Analytical Software (NanoSight, Amesbury, England). The samples were diluted (4000 x - Milli Q[®] water or PBS ~ 7.4 and 5.0) and injected into the sample chamber with a syringe (25°C). The NTA apparatus combines light scattering microscopy with a laser diode (635 nm) camera charge-coupled device, which allows viewing and recording of the NPs in solution. Each video clip was captured over 60 s. The NTA software is able to identify and track individual NPs (10 - 1000 nm), which are in Brownian motion, and relate this particle movement to a sphere with an equivalent R_H , as calculated using the Stokes-Einstein relation (4). The size distribution was expressed by the Span value, which was calculated using Eq. (5).

$$\text{Span} = \frac{d_{(0.9)} - d_{(0.1)}}{d_{(0.5)}} \quad (5)$$

where $d_{(0.9)}$, $d_{(0.1)}$ and $d_{(0.5)}$ are the diameters at 90%, 10% and 50% cumulative volumes, respectively.

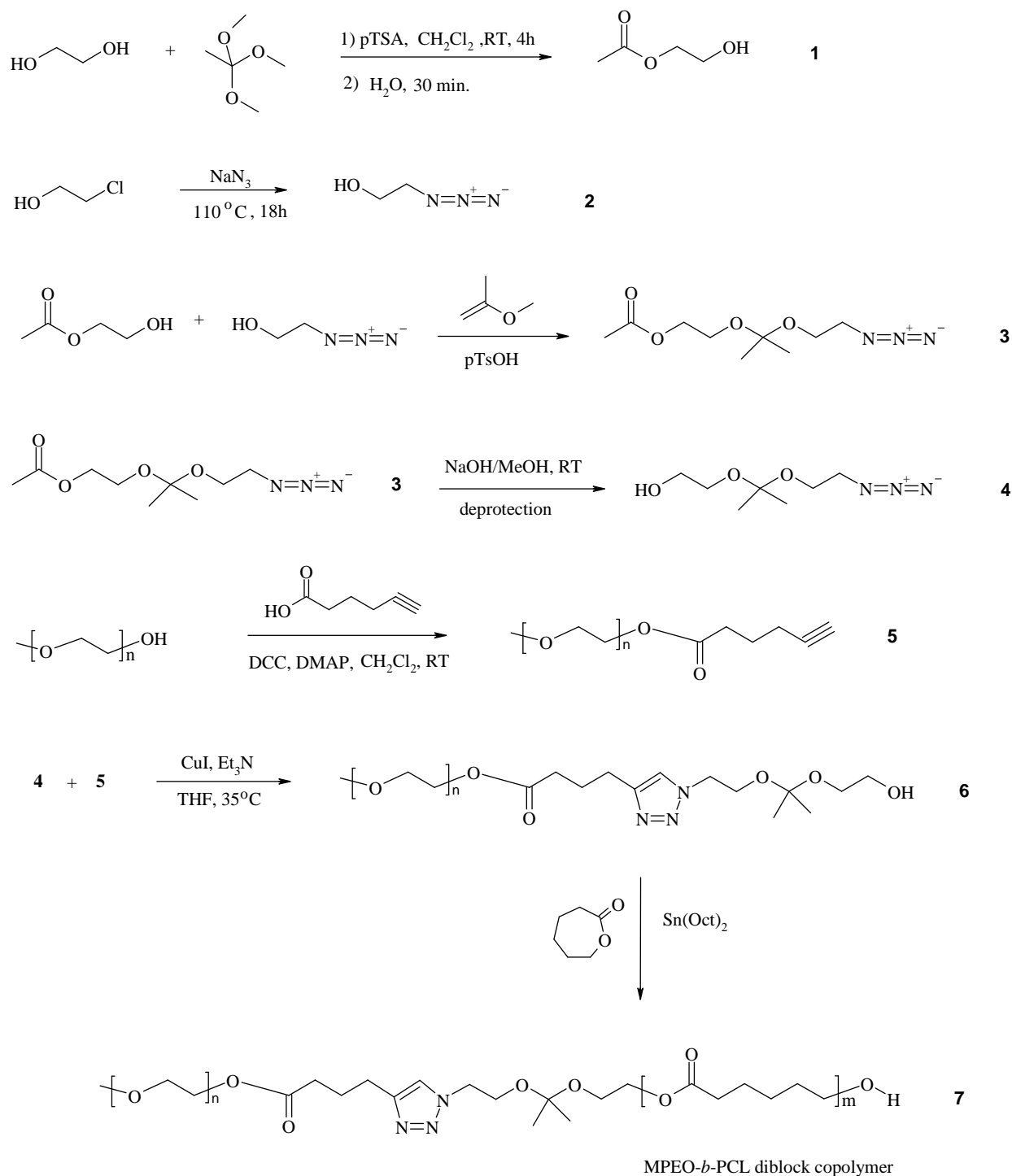
Transmission electron microscopy (TEM)

TEM observations were performed on a Tecnai G2 Spirit Twin at 120 kV (FEI, Czech Republic). The NPs were diluted 100-fold, and $2 \mu\text{L}$ of the aqueous solution was dropped onto a copper TEM grid (300 mesh) coated with thin, electron-transparent carbon film. The solution was removed by touching the bottom of the grid with filter paper. This rapid removal of the solution was performed after 1 min to minimise oversaturation during the drying process; this step was found to be necessary to preserve the structure of the NPs. The NPs were negatively stained with uranyl acetate ($2 \mu\text{L}$ of a 1 wt.% solution dropped onto the dried NPs and removed after 15 s in the same manner described above). The sample was left to completely dry at ambient temperature and then observed via TEM using bright-field imaging. Under these conditions, the micrographs displayed a negatively stained background with bright spots, which correspond to the investigated NPs.

Results and discussion

A new synthetic pathway was developed to obtain well-defined amphiphilic copolymers that contain acid-labile, degradable ketal linkages as block linkers that are highly sensitive to pH under physiological conditions. The synthesis of the biocompatible, biodegradable, acid-labile MPEO-*b*-PCL was designed using, for the first time, the combination of a "click"

reaction with DCC chemistry and ROP (**Scheme 1**). This strategy provides new insights into the combination of new "click" chemistry reactions with the classic synthetic pathways in polymer chemistry.



Scheme 1. Synthetic route for the preparation of MPEO-*b*-PCL diblock copolymers.

Synthesis of compounds 1 to 5

The compounds ethylene glycol monoacetate (**1**)^{44,45} (Fig. S1), 2-azidoethanol (**2**)⁴⁶ (Fig. S2), 2-[[2-(2-azidoethoxypropan-2-yl)oxy]ethyl acetate (**3**)⁴⁵ (Fig. S3), 2-[[2-(2-azidoethoxy)propan-2-yl]ethan-1-ol (**4**)⁴⁵ (Fig. S4) and α -methoxy- ω -alkyne-poly(ethylene oxide) (**5**)⁴⁷ (Fig. S5) were synthesised according to previous reports and were characterised using ¹H and ¹³C NMR, FT-IR spectroscopy and SEC analysis (**5**), which are described in detail in the Supplementary Information.

Synthesis of α -methoxy- ω -hydroxy-poly(ethylene oxide) containing a ketal group (compound **6**):

The α -methoxy- ω -hydroxy-poly(ethylene oxide) containing a ketal group (**6**) was prepared as a macroinitiator through a “click” reaction between α -methoxy- ω -alkyne-PEO (**5**) and 2-[[2-(2-azidoethoxy)propan-2-yl]ethan-1-ol (**4**) (see Scheme 1). The azide-alkyne Huisgen cycloaddition was performed in the presence of CuI and Et₃N. After purification, the obtained macroinitiator was characterised using ¹H and ¹³C NMR, FT-IR spectroscopy and SEC analysis. The ¹H NMR spectrum (Fig. 1, top) confirms that the “click” reaction was complete due to the disappearance of the characteristic signal for the alkyne end-group at $\delta = 1.96$ ppm (**h**) (Fig. S5) and the appearance of a new proton signal from the triazole ring at $\delta = 7.40$ ppm (**h**) in Fig. 1 (top). The signal observed at $\delta = 1.28$ ppm (**j + j'**) is assigned to the six protons of the dimethyl ketal group –OC(CH₃)₂–O– and demonstrates that the ketal group remains unaffected during the azide-alkyne Huisgen cycloaddition. Furthermore, a singlet signal attributed to CH₃–O– was observed at $\delta = 3.39$ ppm (**a**), and other signals were observed at $\delta = 2.76$ ppm (**g**), $\delta = 2.39$ ppm (**e**) and $\delta = 1.96$ ppm (**f**). Additional signals located in the vicinity of the EO ($\delta = 3.63$ ppm) were also identified: $\delta = 2.85$ ppm (**e**) is typical signal of –CH₂–CH₂–O–C(O), $\delta = 4.21$ ppm (**i + i'**) is attributed to –N–CH₂–CH₂–O–, and $\delta = 4.47$ ppm (**d**) is characteristic of –CH₂–CH₂–O–C(O). The conversion of the “click” reaction was calculated from the relative intensities of the signals characteristic of both –O–C(CH₃)₂–O– (**j + j'**, $\delta = 1.28$ ppm) and –CH₂–O–C(O) (**d**, $\delta = 4.47$ ppm) groups in the ¹H NMR spectrum, which gives a quantitative value of ~82%.

Table 1. Macromolecular characteristics of functional MPEO.

MPEO samples	Conversion ^a (%)	M_n^b (¹ H NMR)	M_n^c (SEC)	M_w/M_n^d (SEC)
MPEO	-	1800	1464	1.23
macromer	87	2200	1710	1.24
macroinitiator	82	2320	1760	1.31

^a Conversion was calculated by ¹H NMR spectroscopy (Figs. S5 and 1, top).

^b M_n was calculated by ¹H NMR spectroscopy according to Eqs. (1) and (2).

^c M_n and ^d M_w/M_n were determined by SEC calibrated with PS standards.

The ¹³C NMR spectrum (Fig. 1, bottom) of the α -methoxy- ω -hydroxy-PEO containing a ketal group is further evidence for the successful achievement of the “click” cycloaddition. Signals corresponding to the dimethyl ketal group at $\delta = 24.32$ ppm (**13**) and from the fully substituted carbon –OC(CH₃)₂–O– at 100.33 ppm (**12**) were clearly observed. Other significant signals were observed at high chemical shifts at $\delta = 122.22$ ppm (**9**) and $\delta = 146.97$ ppm (**8**), which correspond to the carbons from the triazole ring –CH₂–CH=CH–N–, and at $\delta = 173.29$ ppm (**4**), which is attributed to the carbonyl carbon from the –CH₂–O–C(O)–(CH₂)₃– group.

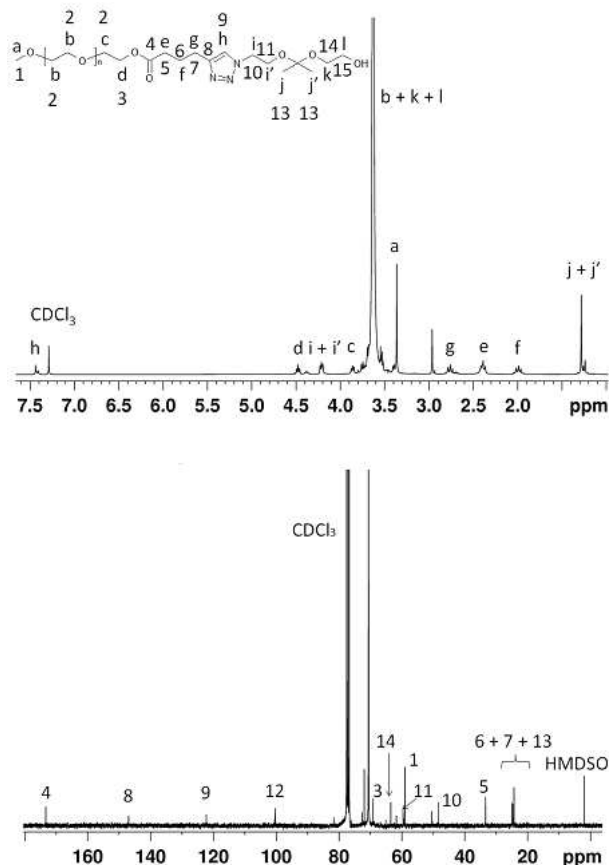


Fig. 1. ¹H (top) and ¹³C (bottom) NMR spectra of the α -methoxy- ω -hydroxy-PEO containing a ketal group in CDCl₃.

Moreover, the effectiveness of the “click” cycloaddition reaction to afford the 1,2,3-triazole as a product was confirmed by FT-IR spectroscopy (Fig. S7, b). Complete disappearance of the peak corresponding to the azide group at 2102 cm⁻¹ was observed, which indicates the completion of the reaction. The identification of C–N stretching frequencies is generally a very difficult task because the mixing of bands is possible in this region.⁵⁰ The absorption bands observed at 1553, 1469 and 1455 cm⁻¹ are due to stretching vibrations between carbon and nitrogen atoms. The characteristic absorption band of C–N observed at 1361 cm⁻¹ confirms the formation of the triazole ring. Absorption bands for the carbon-hydrogen groups were also observed, thus resulting in C–H stretching absorption in the 2992 to 2700 cm⁻¹ region of the IR spectrum. Moreover, in the spectrum of compound **6**, a weak –C=O stretching band at 1735 cm⁻¹ was observed, indicating the presence of a carbonyl ester group. Furthermore, distinctive bands from the ether groups of the EO repeating units at 1107 cm⁻¹ were also observed (Fig. S7, b). The SEC chromatogram from the corresponding macroinitiator obtained after the cycloaddition reaction shows a monomodal distribution, as indicated by the overlap of the SEC traces (dotted line in Fig. S8). The molecular weight of the resulting product remains unchanged, except for a slight increase in polydispersity. Nevertheless, after the reaction, the SEC chromatogram from α -methoxy- ω -hydroxy-MPEO containing a ketal group (**6**) clearly demonstrates the absence of side products with higher M_n values that could be formed as a result of alkyne homocoupling.

Synthesis of MPEO-*b*-PCL diblock copolymer containing a ketal group (compound 7)

The MPEO-*b*-PCL diblock copolymers (**7**) were successfully synthesised by ROP from the ϵ -CL monomer. The previously synthesised α -methoxy- ω -hydroxy-poly(ethylene oxide) containing a ketal group (**6**) was used as a macroinitiator in the presence of Sn(Oct)₂ as a catalyst. The lengths of the PCL blocks were controlled by regulating the ϵ -CL/macroinitiator molar ratio. After purification, the MPEO-*b*-PCL diblock copolymers were characterised using ¹H and ¹³C NMR, FT-IR spectroscopy and SEC analysis. The structure and composition of the obtained diblock copolymers were also confirmed by FT-IR spectroscopy. The ¹H NMR spectrum of the diblock copolymer (**Fig. 2, top**) shows characteristic signals for protons belonging to ϵ -CL and EO repeating units. The signals for the methylene protons of the ϵ -CL units were detected at $\delta = 4.06$ ppm (**r**) –CH₂-OC(O)-, $\delta = 2.29$ ppm (**m**) –C(O)CH₂-, $\delta = 1.58$ ppm (**n + p**) –C(O)-CH₂-CH₂-CH₂-CH₂- and $\delta = 1.34$ ppm (**o**) –C(O)-CH₂-CH₂-. The methylene protons of the EO repeating units were observed at $\delta = 3.63$ ppm (**b**), whereas the singlet signal attributed to the CH₃-O- appeared at $\delta = 3.39$ ppm (**a**). The signal observed at $\delta = 1.31$ ppm (**j + j'**) attributed to the six protons of the dimethyl ketal group –OC(CH₃)₂-O- and the resonance signal at $\delta = 7.37$ ppm (**h**) assigned to the triazole ring demonstrate that the ketal group and the triazole ring remain unaffected following the ROP. Furthermore, there were signals in the spectrum at $\delta = 4.57$ ppm (**l**), attributed to methylene protons from the –CH₂-O-C(O)- fragment; at $\delta = 4.45$ ppm (**d**), assigned to the last monomer unit of PEO; and at $\delta = 4.21$ ppm (**i + i'**), attributed to the methylene protons from the fragment between the triazole ring and the ketal group –N-CH₂-CH₂-O-C(CH₃)₂-O-. Low intensity signals at $\delta = 2.76$ ppm (**g**), 2.50 ppm (**e**) and 2.00 ppm (**f**) for the protons from the –OC(O)-CH₂-CH₂- triazole ring were also present. The experimental degree of ϵ -CL polymerisation agrees well with the theoretical values (**Table 2**). The ¹³C NMR spectrum (**Fig. 2, bottom**) of the diblock copolymers shows carbon signals that are consistent with the desired structure. The most important carbon signals are highlighted, i.e., the signals that correspond to carbons from the dimethyl ketal group at $\delta = 24.39$ ppm (**13**) and the quaternary carbon from the same group –OC(CH₃)₂-O- at $\delta = 121.50$ ppm (**12**). Other significant signals were observed at higher frequencies and slightly shifted in comparison with the ¹³C NMR spectrum from α -methoxy- ω -hydroxy-PEO containing a ketal (**6**) (**Fig. 1, bottom**). These signals appear at $\delta = 147.44$ ppm (**9**) and $\delta = 161.1$ ppm (**8**) for the triazole ring –CH₂-CH=CH-N- and at $\delta = 173.58$ ppm (**4 + 16**) for the carbon from the carbonyl group –CH₂-O-C(O)-(CH₂)₃- next to PEO and for the carbon from carbonyl group in PCL. All of the other remaining signals are attributed to the carbon atoms from the diblock copolymer structure.

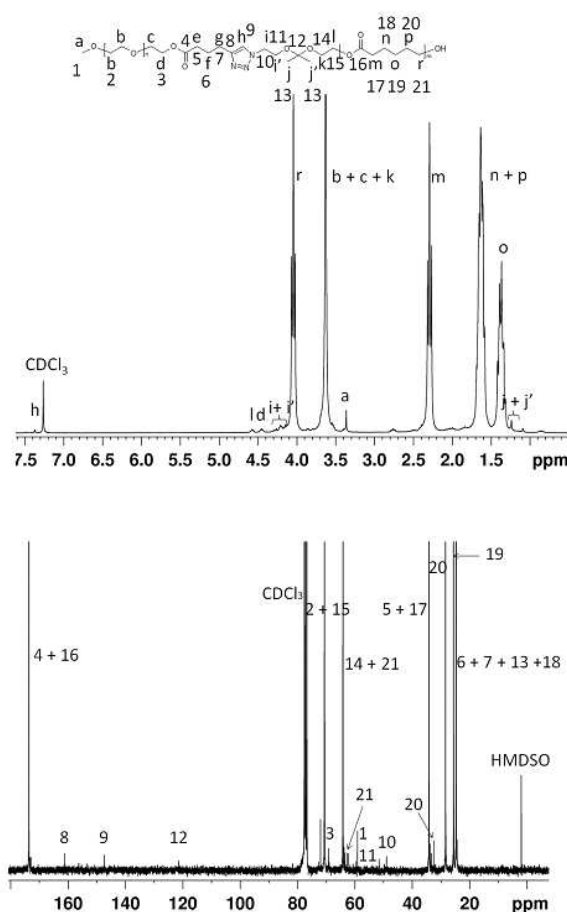


Fig. 2. ¹H (top) and ¹³C (bottom) NMR spectra of the MPEO-*b*-PCL diblock copolymer in CDCl₃.

Similar bands for the characteristics peaks were found for all samples in the FT-IR spectra (**Fig. S7, c**).

Table 2. Macromolecular characteristics of MPEO-*b*-PCL diblock copolymers.

Sample	M_n^a ,(NMR)	M_n^b ,(NMR)	M_n^c ,(SEC)	M_w/M_n^d (SEC)
MPEO ₄₄ - <i>b</i> -PCL ₁₇	4000	5400	3130	1.45
MPEO ₄₄ - <i>b</i> -PCL ₄₄	7000	6830	7570	1.43

^a M_n was calculated by the monomer conversion; $M_n = [M]_0/[I]_0 \times 114 + M_n \alpha$ -methoxy- ω -hydroxy-MPEO containing a ketal group (**6**).

^b M_n was calculated by ¹H NMR spectroscopy according to Eq. (2).

^c M_n and ^d M_w/M_n values relative to PS standards.

The molecular weights and polydispersity indices of the synthesised MPEO-*b*-PCL diblock copolymers were determined by SEC. The analysis clearly shows that the obtained curves are monomodal, confirming that the ketal group was not degraded during the ROP of ϵ -CL. A slight asymmetry is observed at longer elution times in the SEC curve (regular line in **Fig. S9**), which strongly suggests that some unreacted MPEO is present. The molecular characteristics of the diblock copolymers are listed in Table 2.

Polymer nanoparticles (NPs)

As a proof-of-concept, polymer NPs were prepared from the block copolymers, and their behaviours under different simulated physiological conditions were evaluated in detail by DLS and NTA. The visual appearance of the colloidal particles immediately after the injection of the MPEO-*b*-PCL block copolymer solutions into water was size-dependent and did not change after the dilution with PBS (pH ~ 7.4) (data not shown). For MPEO₄₄-*b*-PCL₁₇, the resulting colloidal solution was fully transparent, whereas the solution was slightly opalescent for the MPEO₄₄-*b*-PCL₄₄ block copolymer. This result is a visual indication that the particles produced by the nanoprecipitation protocol using the MPEO₄₄-*b*-PCL₄₄ block copolymer are larger than the particles produced using the MPEO₄₄-*b*-PCL₁₇ block copolymer.⁵¹ **Fig. 3** shows the distribution of R_H for MPEO₄₄-*b*-PCL₁₇ and MPEO₄₄-*b*-PCL₄₄ block copolymer micelles after the dialysis process and dilution with PBS, as measured by DLS. The distribution of R_H for MPEO₄₄-*b*-PCL₁₇ appears as only one single distribution of R_H relative to the presence of the polymer micelles in PBS solution with an average of $R_H = 32.1$ nm (**Fig. 3, blue circles**). Furthermore, the polydispersity of the MPEO₄₄-*b*-PCL₁₇ micelles is very low as estimated through the cumulant analysis ($\mu/I^2 = 0.08 \pm 0.007$). However, for the MPEO₄₄-*b*-PCL₄₄ block copolymer, a bimodal distribution of R_H was observed with average sizes of $R_H = 18.5$ nm and 99.5 nm, respectively (**Fig. 3, red circles**). Because the ketal linkage does not affect the physico-chemical properties of the MPEO-*b*-PCL diblock copolymers, the main factors that control the particle size and morphology in crystalline amphiphilic block copolymers that self-assemble in water are the preparation methodology and the polymer properties, such as the molecular weight and the relative block length.⁵² Although the study of the particles' morphology is far beyond the scope of the current investigation, some comparisons with the literature data could be performed. Similar particle sizes were found in a previous work for micelles of the PEO-*b*-PCL diblock copolymer with the same block length prepared through the dialysis method.^{53,54} For the PEO₄₄-*b*-PCL₄₄ diblock copolymer, mixtures between spherical and cylindrical micelles were found to coexist after dialysis when observed by TEM.⁵³ Spherical micelles with diameters in the range of 35 ± 5 nm were observed concomitantly with cylinders with a broad size range (greater than 100 nm) and polydispersity. Similar results were obtained by others authors⁵⁵ by using the same block and block lengths. The observed bimodal size distribution of R_H for the PEO₄₄-*b*-PCL₄₄ block copolymer is related to a morphological mixture of at least two types of particles. According to the aforementioned literature, the most probable morphological structures are the mixture between spherical micelles with an average size of $D_H = 37.0$ nm and cylindrical and/or worm-like micelles with $D_H = 199$ nm. On the other hand, for PEO₄₄-*b*-PCL₁₇ block copolymer assemblies, single monodisperse spherical micelles are obtained in most cases.

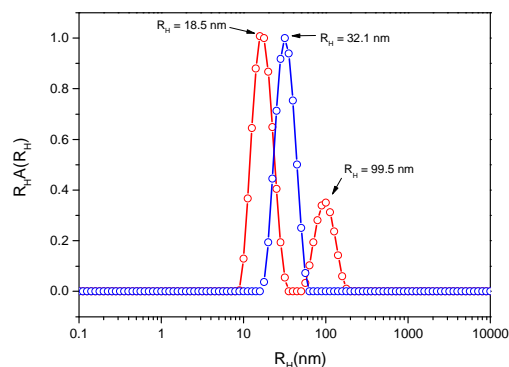


Fig. 3. Distributions of R_H for (○) MPEO₄₄-*b*-PCL₁₇ and (◐) MPEO₄₄-*b*-PCL₄₄ NPs prepared using the nanoprecipitation protocol and diluted in PBS (pH ~ 7.4), both at a concentration of 1 mg.mL⁻¹.

Note that thermodynamically stable polymeric NPs with hydrodynamic diameters ($2R_H = D_H$) within the range of 20 to 60 nm have been shown to be ideal for tumour drug-delivery applications.⁵⁶ They are within the size range that enables renal clearance to be avoided ($D_H > 10$ nm), thereby providing the NPs a potentially prolonged blood circulation time and, considering that their size is below the cut-off size of the leaky pathological vasculature ($D_H < 200$ nm), specific accumulation in solid tumour tissue due to the enhanced permeation and retention (EPR) effect.⁵⁷ Moreover, in addition to the role of the particle size in the EPR effect, another important aforementioned target in cancer therapy is the acidic cytosolic or endosomal conditions in tumour cells. Therefore, the sensibility of the polymer NPs containing the acid-labile ketal group was tested by DLS in acidic media (pH ~ 5) under physiological conditions (37 °C) using the MPEO₄₄-*b*-PCL₁₇ block copolymer. MPEO₄₄-*b*-PCL₁₇ block copolymer NPs were chosen for evaluating the ketal linkage sensibility in vitro because they presented a monodisperse single distribution of R_H with a $D_H = 64.2$ nm, which is within the optimal size for drug-delivery applications. As shown in **Fig. 3**, the absence of a mixture between distinct morphological structures facilitates the experimental procedures and data analysis. **Fig. 4** shows the distribution of R_H for the MPEO₄₄-*b*-PCL₁₇ block copolymer NPs at pH ~ 5.0 and 37 °C as a function of time.

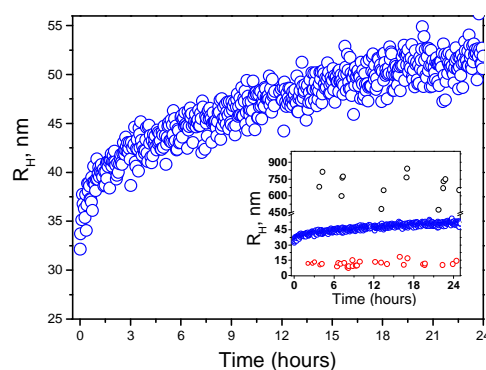


Fig. 4. Temporal dependence on the R_H distribution of MPEO₄₄-*b*-PCL₁₇ NPs at pH ~ 5.0 and 37 °C. The inset illustrates the R_H distribution as a function of time for (○) aggregate NPs, (◐) free PEG chains and (○) loose aggregates.

The results clearly show an increase in the average size of the micellar NPs from $R_H = 32.1$ nm to R_H 52.6 nm in 24 hours, which corresponds to an increase in D_H of approximately 41 nm. To obtain a thorough size distribution and to gain more information to accurately analyse the distribution of monodisperse and polydisperse samples than can be obtained through DLS,^{58,59} the MPEO₄₄-*b*-PCL₁₇ NPs were analysed using NTA at 25 °C. This technique is a powerful tool that complements DLS, and it is particularly valuable for the detection and accurate sizing of a broad range of population ratios. After 24 hours, the MPEO₄₄-*b*-PEO₁₇ block copolymer NPs showed mean particle sizes of 96 nm and 118 nm under pH ~ 7.4 and pH ~ 5.0, respectively. **Fig. 5** depicts the size distributions for the NPs, in which the value of $d(0.1)$ was 64 nm, $d(0.5)$ was 92 nm and $d(0.9)$ was 128 nm (pH ~ 7.4) and $d(0.1)$ was 61 nm, $d(0.5)$ was 92 nm and $d(0.9)$ was 209 nm (pH ~ 5.0). According to Eq. (2), these cumulative volumes give Span values of 0.69 and 1.57 for pH ~ 7.4 and pH ~ 5.0, respectively.

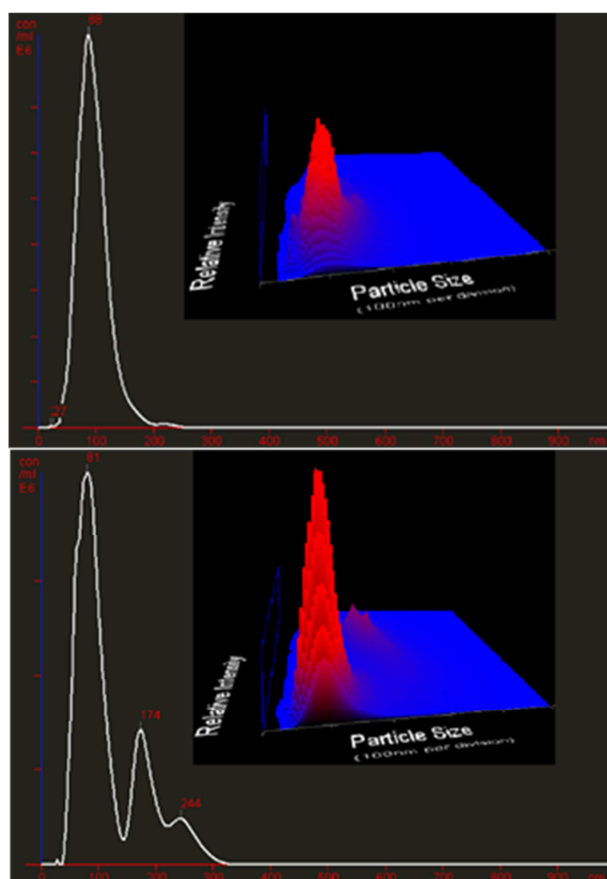


Fig. 5. Size distribution from NTA for the MPEO₄₄-*b*-PCL₁₇ NPs under pH ~ 7.4 (upper) and pH ~ 5.0 (bottom) after 24 h.

In addition, it is possible to verify for the MPEO₄₄-*b*-PEO₁₇ block copolymer NPs the presence of only one sharp peak at pH ~ 7.4 (**Fig. 5, upper**) and three peaks at pH ~ 5.0 (**Fig. 5 bottom**). Similarly, the TEM images (**Fig. 6**) showed a comparable increase in the size of the MPEO₄₄-*b*-PEO₁₇ block copolymer NPs at pH ~ 5.0 (**Fig. 6, b**) when compared to the NPs at pH ~ 7.4 (**Fig. 6, a**) after 24 hours. The particle sizes determined from the TEM images are clearly smaller than those determined using scattering techniques. This discrepancy can

be explained by a combination of two effects: (i) during sample preparation, the particles undergo dehydration and may shrink, and (ii) scattering techniques report an intensity-average dimension, whereas TEM reports a number-average dimension. Therefore, TEM images generally yield smaller sizes relative to DLS data.⁶⁰

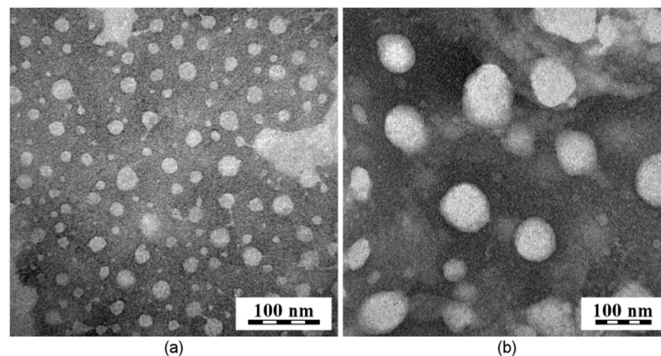


Fig. 6. TEM images of MPEO₄₄-*b*-PCL₁₇ NPs at pH ~ 7.4 (a) and at pH ~ 5.0 (b) after 24 h.

The increases in particle size and size distribution, as shown by both scattering techniques and TEM, are strong evidence for micellar aggregation over time. The aggregation mechanism could be explained through the hydrolysis of the acid-labile ketal linkage in the MPEO₄₄-*b*-PCL₁₇ block copolymer micelles at pH 5.0. While the hydrolysis of the ketal occurs at the interface between the PCL core and the PEG shell inside the micelles, the free hydrolysed PEG chains begin to be released into the media (inset, **Fig. 4**). The decrease in the density of surface PEG chains leads to a decrease in the steric hindrance of the particles and to an increase in the hydrophobicity of the particles, and consequently, particle aggregation.²³ The linear relationship observed between the relaxation rates (I) and the square of the wave vector (q^2) for the particles before (37 °C and pH ~ 7.4) and after 24 hours (37 °C and pH ~ 5.0) demonstrates that both NPs and their aggregates are spherical (**Fig. S10** and **Fig. 6**), and no distinct micellar structures were observed by DLS, NTA and TEM. Furthermore, no changes in the particle size distributions were observed for the MPEO₄₄-*b*-PCL₁₇ block copolymer micelle by DLS at pH ~ 7.4 during 24 hours, confirming that the particles are selective to environments with mild acidic conditions (from pH ~ 5 to ~ 6.5) such as tumour tissues (**Fig. S11**). Moreover, the degradation of the MPEO₄₄-*b*-PCL₁₇ diblock copolymer was confirmed by ¹³C NMR spectroscopy. For the NMR study, 40-50 mg of the MPEO₄₄-*b*-PCL₁₇ diblock copolymer was dissolved in 0.6 mL of deuterated chloroform followed by the addition of 25 μL of hydrochloric acid-d (DCI). The degradation was determined based on the disappearance of the signal from the ketal linkage between the PEO and PCL blocks. **Fig. S12** shows the ¹³C NMR spectra of the MPEO₄₄-*b*-PCL₁₇ copolymer (a) before and (b) after the addition of DCI. The ¹³C NMR spectra reveal the complete disappearance of the carbon signal from the ketal group linker -OC(CH₃)₂-O- at $\delta = 121.50$ ppm (**12, Fig. S12**) after the addition of DCI (**12, Fig. S12, b**). This observation is strong evidence that hydrolytic degradation occurs in the ketal linkage of the MPEO₄₄-*b*-PCL₁₇ diblock. Unfortunately, the usual degradation products resulting from the acid hydrolysis of a ketal group, such as acetone,²⁷ could not be detected in the ¹³C-NMR spectrum. Their signal is hidden under that of the ϵ -CL repeating units in the ¹³C NMR. According to the ¹³C NMR spectra, no changes were observed

in the signal from ϵ -CL repeating units after the addition of DCI. The signals from the methylene carbons $-\text{CO}-(\text{CH}_2)_5-\text{O}$ (**17** to **21** from $\delta = 20$ to $\delta = 65$ ppm, **Fig. S12**) and from the carbonyl group (**16** at $\delta = 173$ ppm, **Fig. S12**) related to the PCL segments remain unchanged. Moreover, no new signal from side products that could derive from the hydrolysis of ester bonds related to the PCL segments was detected after the acid addition. However, a visible decrease in the methylene signal $-\text{O}-(\text{CH}_2)_2-\text{O}$ (**2** at $\delta = 70$ ppm, **S12, b**) related to MPEO units was observed in the ^{13}C NMR spectra. The decrease in the signal of the MPEO units is related to the experimental procedures. After the addition of DCI to the MPEO₄₄-*b*-PCL₁₇ block copolymer solution in CDCl₃, the NMR tube was vigorously shaken. The formation of an emulsion composed of droplets of D₂O containing the MPEO blocks dissolved in (internal phase) and the PCL blocks dissolved on the outer phase (CDCl₃, organic phase) spontaneously occurs. While hydrolysis of the ketal group occurs, the released PCL segments are dissolved in the outer organic phase (CDCl₃), whereas the MPEO blocks remain dissolved in the emulsion droplets (D₂O) with restricted mobility. The restriction in the mobility of the MPEO chains dissolved in the D₂O droplets decreases the signal intensity in the ^{13}C NMR spectra.⁶¹

Conclusions

Through the combination of carbodiimide chemistry and ROP mechanisms with a “click” reaction, novel pH-sensitive amphiphilic block copolymers containing acid-labile ketal groups as block linkers were successfully synthesised using a multi-step stage-by-stage synthetic strategy. The acid-cleavable linkage in the block copolymer backbone was used as a junction point for the design of hydrophilic PEO and hydrophobic PCL segments. For this purpose, a 2-[[2-(2-azidoethoxy)propan-2-yl]]ethan-1-ol compound, with a specific degradable linkage (acyclic ketal group), was synthesised for the first time. Subsequently, α -methoxy- ω -hydroxy-PEO containing a ketal group was prepared as a macroinitiator through a “click” reaction between previously synthesised α -methoxy- ω -alkyne-PEO and 2-[[2-(2-azidoethoxy)propan-2-yl]]ethan-1-ol. The obtained macroinitiator was applied for the sequential controlled ROP of ϵ -CL in the presence of Sn(Oct)₂. Different ratios of ϵ -caprolactone/hydroxyl were used to obtain copolymers with different PCL block lengths. Good control, purity and conversion over each obtained product were achieved without degradation of the acid-labile ketal group. Upon dissolution in a mild organic solvent, the MPEO₄₄-*b*-PCL₁₇ block copolymer self-assembled in water/PBS into regular spherical NPs, and the presence of the acid-labile ketal group linker allowed the NPs to disassemble and aggregate in buffer that simulated acidic cytosolic or endosomal conditions in tumour cells (pH ~ 5.0), as evaluated by DLS and NTA analyses and TEM images. The synthesised block copolymers could be used in a variety of applications, e.g., as pH-triggered release drug-delivery systems.

Acknowledgements

This research was supported by the Grant Agency of the Czech Republic (P208/10/1600). E.J., R.K., and A.J. acknowledge Charles University (Prague, CZ) for the financial support and for the opportunity to pursue their Ph.D. studies. C. G. Venturini acknowledges the Program Science Without Borders CAPES/Brazil (Process number 2293/13-7). The electron microscopy was supported through grant TACR TE01020118.

Notes

Institute of Macromolecular Chemistry v.v.i., Academy of Sciences of the Czech Republic, Heyrovsky Sq. 2, 162 06 Prague 6, Czech Republic.

E-mail: petrova@imc.cas.cz; Tel: +420 296 809 296.

Electronic Supplementary Information (ESI) available: [details of any supplementary information available should be included here]. See DOI: 10.1039/b000000x/

References

- 1 Y.-Y. Won, H.T. Davis, F.S. Bates, *Science* 1999, **283**, 960-963.
- 2 J.K. Kim, E. Lee, Z.G. Huang, M. Lee, *J. Am. Chem. Soc.*, 2006, **128**, 14022-14023.
- 3 E. Busseron, Y. Ruff, E. Moulin, N. Giuseppone, *Nanoscale* 2013, **5**, 7098-7140.
- 4 D.E. Cola, C. Lefebvre, A. Deffieux, T. Narayanan, R. Borsali, *Soft Matter*, 2009, **5**, 1081-1090.
- 5 A.H. Gröschel, F.H. Schacher, H. Schmalz, O.V. Borisov, E.B. Zhulina, A. Walther, A.H.E. Müller, *Nat. Commun.*, 2012, **3**, 1-11.
- 6 T. Smart, H. Lomas, M. Massgnani, M.V. Flores-Merino, L.R. Perez, G. Battaglia, *Nano Today* 2008, **3**, 38-46.
- 7 R.B. Grubbs, Z. Sun, *Chem. Soc. Rev.*, 2013, **42**, 7436-7445.
- 8 X.-B. Xiong, A. Falamarzian, S.M. Garg, A. Lavasanifar, *J. Control. Release* 2011, **155**, 248-261.
- 9 W. Shao, K. Miao, H. Liu, C. Ye, J. Du, Y. Zhao, *Polym. Chem.*, 2013, **4**, 3398-3410.
- 10 W. Wang, H. Sun, F. Meng, S. Ma, H. Liu, Z. Zhong, *Soft Matter*, 2012, **8**, 3949-3956.
- 11 W.J. Li, C.T. Laurencin, E.J. Caterson, R.S. Tuan, K.K. Frank, *J. Biomed. Mater. Res.*, 2001, **60**, 613-621.
- 12 W.J. Li, K.G. Danielson, P.G. Alexander, R.S. Tuan, *J. Biomed. Mater. Res A*, 2003, **67**, 1105-1114.
- 13 C. Drew, X. Wang, L.A. Samuelson, J. Kumar, *J. Macromol. Sci. Pure Appl. Chem.* 2003, **40**, 1415-1422.
- 14 S.V. Trubetskoy, *Adv. Drug Del. Rev.*, 1999, **37**, 81-88.
- 15 V.P. Torchilin, *Coll. Surf. B Biointerfaces* 1999, **16**, 305-319.
- 16 K. Miyata, N. Nishiyama, K. Kataoka, *Chem. Soc. Rev.*, 2012, **41**, 2562-2574.
- 17 J.H. Jeong and T.G. Park, *J. Control. Release* 2002, **82**, 159-166.
- 18 Y. Ymamoto, Y. Nagasaki, Y. Kato, Y. Sugiyama, K. Kataoka, *J. Control. Release* 2001, **77**, 27-38.
- 19 A. Rösler, G.W.M. Vandermeulen, H.-A. Klok, *Adv. Drug Del. Rev.*, 2001, **53**, 95-105.
- 20 Q. Zhang, N.R. Ko, J.K. Oh, *Chem. Comm.*, 2012, **48**, 7542-7552.
- 21 E.G. Kelley, J.N.L. Albert, M.O. Sullivan, T.H. Epps, *Chem. Soc. Rev.*, 2013, **42**, 7057-7071.
- 22 S. Binauld, M.H. and Stenzel, *Chem. Comm.*, 2013, **49**, 2082-2102.
- 23 F.C. Giacomelli, P. Stepánek, C. Giacomelli, V. Schmidt, E. Jäger, A. Jäger, K. Ulbrich, *Soft Matter*, 2011, **7**, 9316-9325.
- 24 S. Mura, J. Nicolas, P. Couvreur, *Nat. Mater.* 2013, **12**, 991-1003.
- 25 E. Jäger, A. Jäger, P. Chytil, T. Etrych, B. Říhova, F.C. Giacomelli, P. Stepánek, K. Ulbrich, *J. Control. Release* 2013, **165**, 153-161.
- 26 I. F. Tannock and D. Rotin, *Cancer Res.*, 1989, **49**, 4373-4384.

- 27 H. Yin, E. S. Lee, D. Kim, K. H. Lee, K. T. Oh and Y. H. Bae, *J. Control. Release* 2008, **126**, 130-138.
- 28 S. Sengupta, D. Eavarone, I. Capila, G. Zhao, N. Watson, T. Kiziltepe, R. Sasisekharan, *Nature* 2005, **436**, 568-572.
- 29 S. Aryal, C.J. Hu, L. Zhang, *ACS Nano* 2010, **4**, 251-258.
- 30 H. Mok, J.W. Park, T.G. Park, *Bioconjugate Chem.*, 2008, **19**, 797-801.
- 31 A.P. Griset, J. Walpole, R. Liu, A. Gaffey, Y.L. Colson, M.W. Grinstaff, *J. Am. Chem. Soc.*, 2009, **131**, 2469-2471.
- 32 B. Wang, C. Xu, J. Xie, Z. Yang, S. Sun, *J. Am. Chem. Soc.*, 2008, **130**, 14436-14437.
- 33 M.M. Ali, M. Oishi, F. Nagatsugi, K. Mori, Y. Nagasaki, K. Kataoka, S. Sasaki, *Angew. Chem. Int. Ed.*, 2006, **45**, 3136-3140.
- 34 Y. Li and P.I Lee, *Int. J. Pharm.*, 2010, **383**, 45-52.
- 35 S.D. Khaja, S. Lee, N. Murthy, *Biomacromolecules* 2007, **8**, 1391-1395.
- 36 J. Siepmann and A. Göpferich, *Adv. Drug Del. Rev.*, 2001, **48**, 229-247.
- 37 J. H. Jeong, S.W. Kim, T.G. Park, *Bioconjugate Chem.*, 2003, **14**, 473-479.
- 38 M.A.R. Meier, S.N.H. Aerts, B.B.P. Staal, M. Rasa, U.S. Schubert, *Macromol. Rapid Commun.*, 2005, **26**, 1918-24.
- 39 S. Petrova, I. Kolev, S. Miloshev, M.D. Apostolova, R. Mateva, *J. Mater. Sci.: Mater. Med.*, 2012, **23**, 1225-1234.
- 40 J. Wu and C-C. Chu, *Acta Biomater.*, 2012, **8**, 4314-4323.
- 41 J. Nicolas, S. Mura, D. Brambila, N. Mackiewicz, P. Couvreur, *Chem. Soc. Rev.*, 2013, **42**, 1147-1235.
- 42 J. Rieger, P. Dubois, R. Jérôme, C. Jérôme, *Langmuir* 2006, **22**, 7471-7479.
- 43 N. Kumar, M.N.V. Ravikumar, A.J. Domb, *Adv. Drug Deliv. Rev.*, 2001, **53**, 23-44.
- 44 M. Oikawa, A. Wada, F. Okazaki, S.J. Kusumoto, *Org. Chem.*, 1996, **61**, 4469-4471.
- 45 R.A. Sheno, B.F.L. Lai, J.N. Kizhakkedathu, *Biomacromolecules* 2012, **13**, 3018-3030.
- 46 O. Norberg, L. Deng, T. Aastrup, M. Yan, *Anal. Chem.*, 2011, **83**, 1000-1007.
- 47 H. Freichels, V. Pourcelle, R. Auzély-Velty, J. Marchand-Brynaert, C. Jérôme, *Biomacromolecules*, 2012, **13**, 760-768.
- 48 P. Štěpánek, *J. Chem. Phys.*, 1993, **99**, 6384-6393.
- 49 J. Jakes, *Czech. J. Phys. Sect B*, 1988, **38**, 1305.
- 50 V. Krishnakumar and J.R. Xavier, *Spectrochim. Acta Mol. Biomol. Spectros.*, 2004, **60**, 709-714.
- 51 A.M. de Oliveira, E. Jäger, A. Jäger, P. Štěpánek, F.C. Giacomelli, *Coll. Surf. A: Physicochemical and Eng. Asp.*, 2013, **436**, 1092-1102.
- 52 A. Choucair and A. Eisenberg, *Eur. Phys. J. E.*, 2003, **10**, 37-44.
- 53 Z.-X. Du, J.-T Xu, Z.-Q. Fan, *Macromolecules* 2007, **40**, 7633-7637.
- 54 P. Schuetz, M. J. Greenall, J. Bent, S. Fuzzeland, D. Atkins, M. F. Butler, T. C. B. McLeishd, D. M. A. Buzzza, *Soft Matter* 2011, **7**, 749-759.
- 55 S.M. Loverde, M.L. Klein, D.E. Discher, *Adv. Mater.*, 2012, **24**, 3823-3830.
- 56 H. Cabral, Y. Matsumoto, K. Mizuno, Q. Chen, M. Murakami, M. Kimura, Y. Terada, M. R. Kano, K. Miyazono, M. Uesaka, N. Nishiyama, K. Kataoka, *Nat. Nanotechnol.*, 2011, **6**, 815-823.
- 57 H. Maeda, H. Nakamura, J. Fang, *Adv. Drug Del. Rev.*, 2013, **65**, 71-79.
- 58 V. Filipe, A. Hawe, W. Jiskoot, *Pharm. Res.*, 2010, **27**, 796-810.
- 59 A.E. James and J.D. Driskell, *Analyst* 2013, **138**, 1212-1218.
- 60 A. Jäger, D. Gromadzki, E. Jäger, F.C. Giacomelli, A. Kozłowska, L. Kobera, J. Brus, B. Řhova, M. El Fray, K. Ulbrich, P. Štěpánek, *Soft Matter*, 2012, **8**, 4343-4354.
- 61 J. Spěvácěk, *Makromol. Chem., Rapid Commun.*, 1982, **3**, 697-703.